Clusters

Small Gold(I) and Gold(I)–Silver(I) Clusters by C–Si Auration

Xiao-Li Pei,[a, b] Ana Pereira,[a, b] Ekaterina S. Smirnova,[a, b] and Antonio M. Echavarren*[a, b]

Abstract: Auration of *o*-trimethylsilyl arylphosphines leads to the formation of gold and gold–silver clusters with *ortho*-metalated phosphines displaying 3c–2e Au–C–M bonds (M = Au/Ag). Hexagold clusters $[Au_6L_4](X)_2$ are obtained by reaction of (L–TMS)AuCl with AgX, whereas reaction with AgX and Ag_2O leads to gold–silver clusters $[Au_4Ag_2L_4](X)_2$. Oxo-trigold(I) species $[Au_3O]^+$ were identified as the intermediates in the formation of the silver-doped clusters. Other $[Au_5]$, $[Au_4Ag]$, and $[Au_{12}Ag_4]$ clusters were also obtained. Clusters containing PAu–Au–AuP structural motif display good catalytic activity in the activation of alkynes under homogeneous conditions.

Introduction

Aurophilicity has a fundamental importance on the wide structural diversity of gold complexes and clusters,[1] as well as on their photophysical properties[2] and their catalytic transformations.[3] Small gold Au_n clusters ($n = 3$–10) can catalyze different reactions[4] and it has been proposed that small gold clusters can activate the C–H bond of methane.[5] However, polynuclear cationic Au^I entities remain nearly unexplored in gold catalysis. To date, only a few catalytically active Au^I_n clusters ($n \geq 3$) have been reported. Thus, the group of Toste found that trinuclear oxonium gold cluster $[(Ph_3PAu)_3O](BF_4)$ is a catalyst for the cycloisomerization of 1,5-allenyenes[6] and our group reported that tetranuclear and pentanuclear gold–silver clusters are active in the catalytic carbonylation of amines under homogeneous conditions.[7]

Ligands play a crucial role in the engineering of gold architectures and the tuning of their properties.[8] The strategy of combining neutral phosphines and anionic ligands such as thiolate/alkynyl ligands[9] has been gaining considerable attention for the construction of hetero-ligated gold clusters, because the higher affinity between gold and anionic fragments allows accessing gold systems of high nuclearity.[10] However, phosphines with both multi-coordination ability and anionic properties have been less explored as ligands for the preparation of gold clusters.

We have described the synthesis of a single example of a hexagold cluster by a Au^I/B transmetalation (Scheme 1 a), which showed catalytic activity in some cycloisomerization of enynes.[11] Now we have developed a more general method by auration-assisted C–Si bond cleavage[12] from *ortho*-silylphosphines gold(I) chloride complexes **1**, which leads to hexanuclear gold(I) clusters $[Au_6L_4](SbF_6)_2$ (**2**) bearing different phosphine L ligands (Scheme 1 b). Interestingly, when the transmetalation was carried out in the presence of Ag_2O, heteronuclear clusters $[Au_4Ag_2L_4](SbF_6)_2$ (**3**) were obtained. All these hexanuclear clusters show 3c–2e Au–C–M bonds (M = Au/Ag).[13] Under slightly different reaction conditions, other polynuclear gold clusters have been also obtained by C–Si auration.

Oxonium trigold clusters $[Au_3O]^+$ were found to be the key intermediates in the formation of gold–silver clusters **3**. Fur-

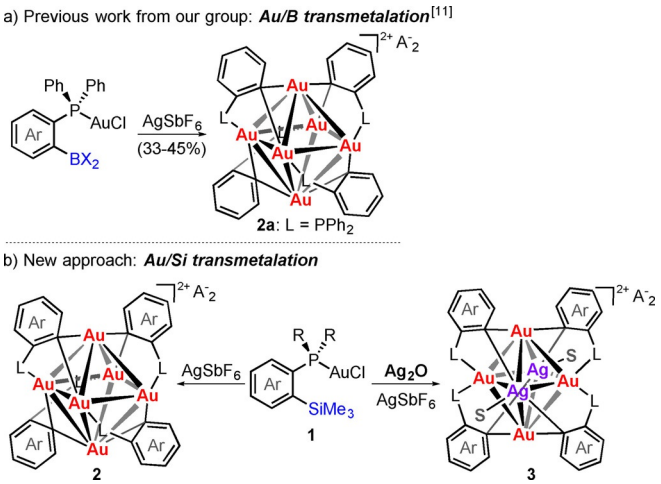

Scheme 1. a) C–B auration to form hexanuclear gold clusters **2a**.[11] b) C–Si auration of *o*-silylphosphine gold(I) complexes **1** to form hexanuclear gold clusters **2** and gold(I)–silver(I) clusters **3**. L = PR_2, A = SbF_6.

[a] Dr. X.-L. Pei, Dr. A. Pereira, Dr. E. S. Smirnova, Prof. A. M. Echavarren
Institute of Chemical Research of Catalonia (ICIQ)
Barcelona Institute of Science and Technology
Av. Països Catalans 16, 43007 Tarragona (Spain)
E-mail: aechavarren@iciq.es

[b] Dr. X.-L. Pei, Dr. A. Pereira, Dr. E. S. Smirnova, Prof. A. M. Echavarren
Departament de Química Analítica i Química Orgànica
Universitat Rovira i Virgili, C/ Marcel·li Domingo s/n
43007 Tarragona (Spain)

Supporting information and the ORCID identification number(s) for the author(s) of this article can be found under: https://doi.org/10.1002/chem.202001509.

thermore, our studies reveal that clusters containing the PAu–Au–AuP structural motif activate alkynes under homogeneous conditions, presumably as a consequence of the presence of coordinatively labile gold(I), similar to gold cavities (pocket-like sites) that exist in the well-studied [Au_{25}] cluster.[3b,14]

Results and Discussion

The *o*-trimethylsilylaryl phosphine gold(I) complexes **1a–e** were prepared in 89–95% yields from the corresponding *o*-trimethylsilylaryl phosphines and [Me_2SAuCl] in CH_2Cl_2 at 23 °C. Complexes **1a–d** react with 1 equivalent of $AgSbF_6$ in MeOH–CH_2Cl_2 to form known **2a**[11] as well as new hexanuclear gold clusters **2b–e**, which were isolated as yellow or pale-yellow crystalline solids in 52–81% yields (Scheme 2).[15] The reaction of complex **1a** with different silver salts AgX (X = BF_4, OTf, NTf_2, NO_3) led to the corresponding $[Au_6(L)_4](X)_2$ clusters. However, other chloride scavengers such as $Cu(OTf)_2$, $Zn(OTf)_2$, $In(OTf)_3$, TMSOTf, or $Sc(OTf)_3$ were not effective. When using $NaBAr^F{}_4$, the corresponding hexanuclear gold species could be observed by ^{31}P NMR.

Complexes **1a–e** derived from triaryl phosphines show singlets in their $^{31}P\{^1H\}$ NMR spectra at 32.3–37.8 ppm in CD_2Cl_2, whereas the corresponding signals for dialkyl(*o*-trimethylsiliylaryl)phosphine and di(2-furyl)(*o*-trimethylsiliylaryl)phosphine gold(I) complexes **1d** and **1e** were observed at 47.10 and −5.12 ppm, respectively. The resulting hexanuclear clusters showed their ^{31}P signals shifted downfield by 8–24 ppm: **2a–c** (44.6–48.2), **2d** (71.50), and **2e** (3.15).

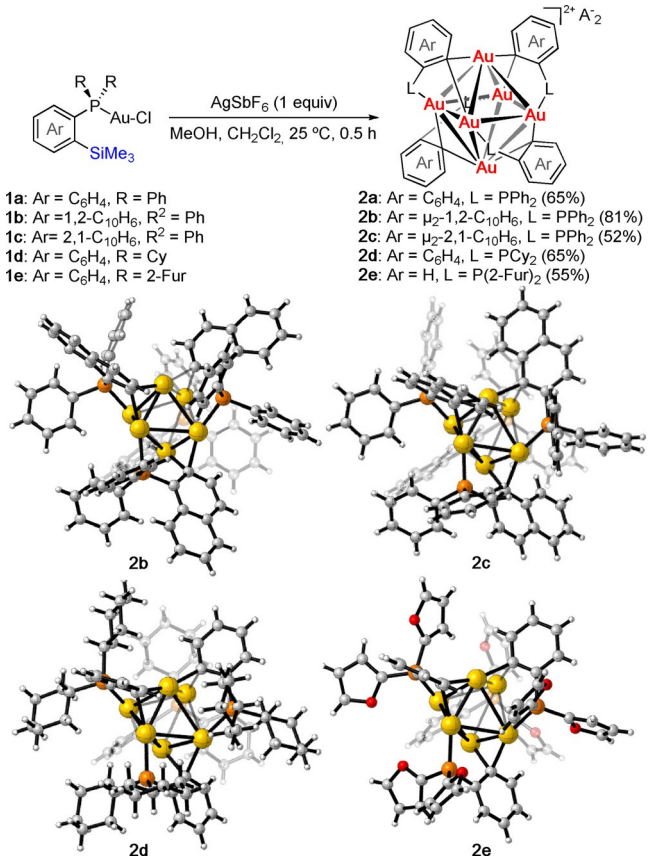

Scheme 2. Hexanuclear gold clusters **2a–e**, obtained by C–Si auration from **1a–e**. A = SbF_6. Fur: furyl. 1,2-$C_{10}H_4$ and 2,1-$C_{10}H_4$ derived from 1-diphenylphosphino-2-trimethylsilylnaphthalene and 2-diphenylphosphino-1-trimethylsilylnaphthalene, respectively. Counteranions and solvent molecules are omitted for clarity.

New clusters **2b–e** were characterized by X-ray diffraction, showing a pseudo-octahedral geometry with six gold atoms stabilized by only four formally anionic-phosphine ligands, different from the hexanuclear gold clusters.[16,17] Compared to aurophilic interactions of 2.706(4)–3.351(4) Å found in **2a**,[11] the Au–Au bonds lie in the range of 2.689(7)–3.162(8) Å in **2b**, 2.718(6)–3.352(6) Å in **2c**, 2.726(4)–3.325(4) Å in **2d**, and 2.709(2)–3.341(2) Å in **2e**, respectively. In clusters **2b–c**, two naphthyl groups stabilize the gold atoms in the 3c–2e Au–C–Au bonds, whereas two phenyl groups are involved in the 3c–2e bonds in clusters **2d–e**. The average C-Au-C angles in **2b** (159.6(6)°) and **2c** (162.1(4)°) are slightly bigger than those of **2a** (159.1(3)°). In clusters **2d** and **2e**, the average C-Au-C angles are 157.8(3) and 162.2°, respectively.[15]

Reaction of **1a** with excess of silver(I) salts did not result in the formation of gold–silver clusters. However, addition of excess $AgSbF_6$ to a suspension of **1a** and 1 equivalent of Ag_2O in CH_2Cl_2 led to the formation of heterometallic cluster **4a** (Scheme 3). Notably, cluster **4a** rearranges in the presence of acetone to form cluster **3a**, in which each of the silver atoms coordinates with a molecule of acetone. Similar behavior was observed in acetonitrile or methanol. Upon removal of the coordinating solvent under vacuum, **3a** was slowly converted into **4a**. Two related gold–silver clusters **3b** and **4c** were also obtained and structurally characterized. In the silver-doped hexanuclear gold–silver clusters **4a** and **4c**, silver atoms substitute the two axial positions, forming 3c–2e Au–C–Ag bonds.[15] Due to the argentophilic interactions in **4a** and **4c** (*ca.* 2.9 Å), the hexanuclear heterometallic cores are distributed as distorted octahedrons with edge-sharing bi-tetrahedral geometry, similar to the structure of hexanuclear nanogold cluster [(*p*-$C_6H_4MeP)_6Au_6](NO_3)_2$.[17] The ligand coordination in **3a** and **3b** is very different. In cluster **3a**, four gold atoms are linked together by the R_2P group and the aryl rings, displaying the same coordinating mode as in hexagold(I) analogues **2a–e**. The structure of **3b** is more distorted and can be viewed as the fusion of two binuclear gold complexes bridged by two silver atoms by Au–Ag interactions.

Clusters **4a** and **4c** display doublets at 46.5 and 40.3 ppm, respectively in the $^{31}P\{^1H\}$ NMR spectra, whereas **3a** and **3b** show triplets at 52.2 and 55.8 ppm, respectively.

Hexadecanuclear heterometallic cluster **5a** was obtained as a byproduct in the preparation of **4a** (Scheme 3). This cluster could also be accessed from a complex [(L)Au(NEt_3)](SbF_6) **1a′**, prepared by reaction of **1a** with $AgSbF_6$ in the presence of excess NEt_3. Treatment of **1a′** in CH_2Cl_2 containing excess water with $AgSbF_6$ (2 equiv) led to **5a** in 47% yield. Cluster **5a′** was prepared similarly using $AgNTf_2$ instead of $AgSbF_6$. The structure of **5a′** shows 3c–2e Au–C–Au and Au–C–Ag bonds, as well as an interesting μ^4-O^{2-} coordinating mode, which to the best of our knowledge, corresponds to the highest-nuclei oxo-bridged gold–silver assembly among the known oxo-gold clusters.[15,18]

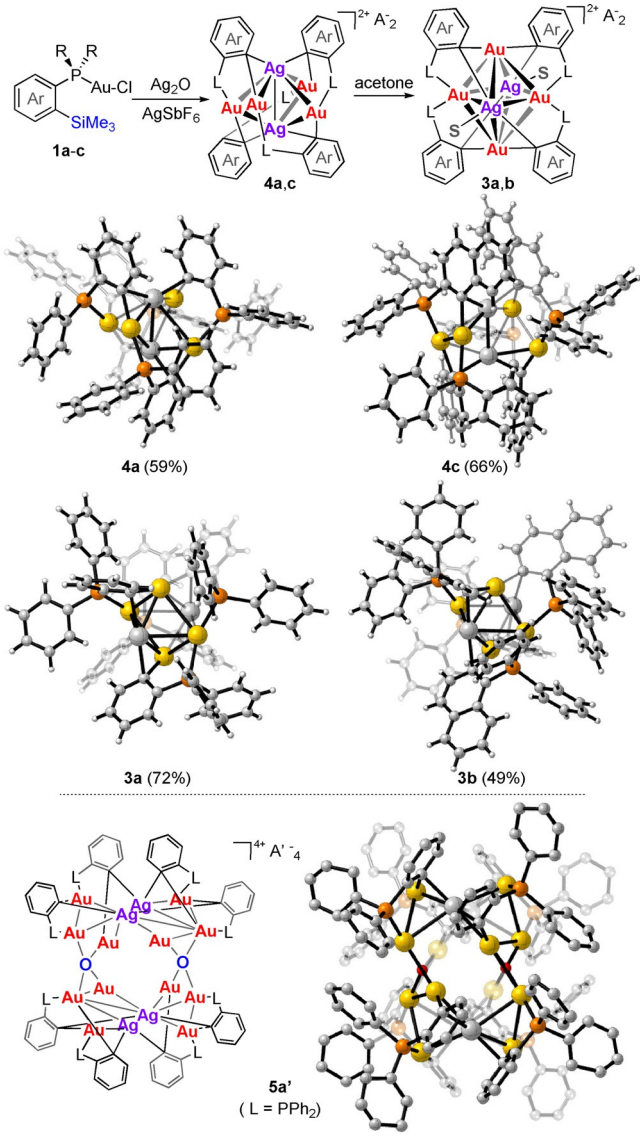

Scheme 3. Hexanuclear gold–silver clusters **3a,b**, **4a,c**, and **5a′** by C–Si auration in the presence of Ag_2O. A = SbF_6, A′ = NTf_2. Hydrogen atoms in **5a'**, counteranions and solvent molecules are omitted for clarity.

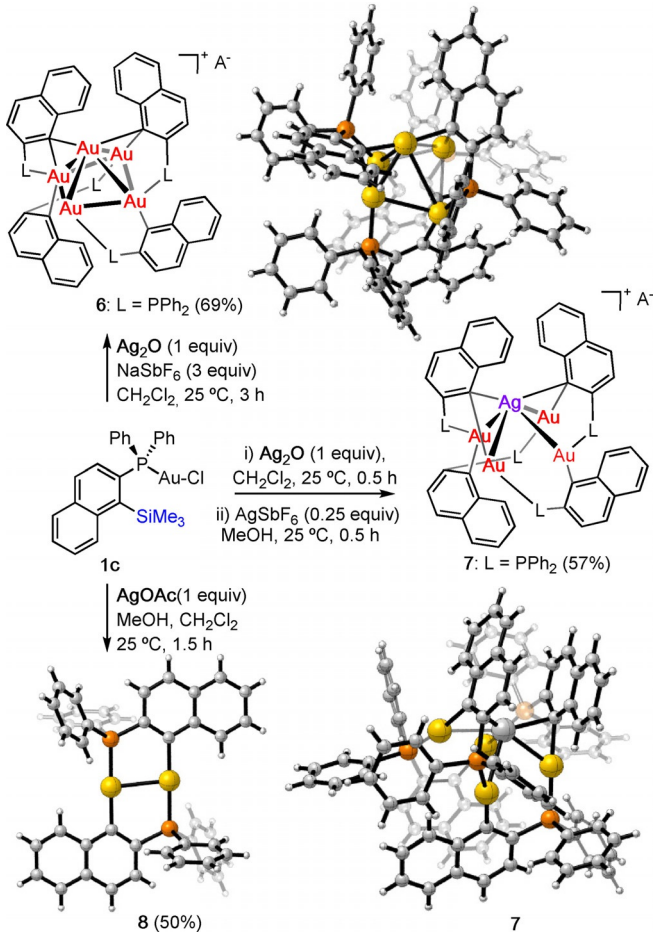

Scheme 4. Clusters **6**–**8** obtained from gold(I) complex **2c**. A = SbF_6. Counteranions and solvent molecules are omitted for clarity.

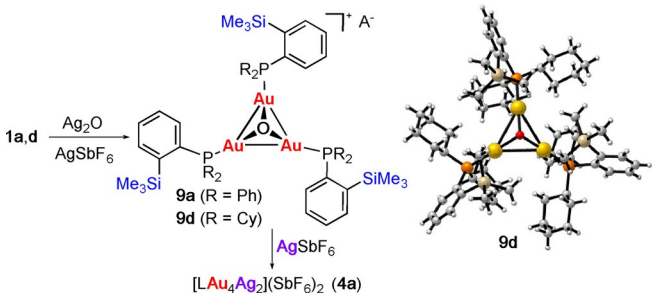

Scheme 5. Oxonium gold intermediates **9a,b** from **1a,d**. A = SbF_6. Counteranions and solvent molecules are omitted for clarity.

Interestingly, treatment of **1c** with $NaSbF_6$ and Ag_2O led to pentanuclear gold(I) cluster **6** in 69% yield,[19] along with pentanuclear gold(I)–silver(I) **7** as a minor product (*ca.* 5%) (Scheme 4). Cluster **7** could be obtained from **1c** in 57% yield using 0.25 equivalents of $AgSbF_6$.[15] Moreover, digold complex[15,20] **8** was obtained by reaction of **1c** with AgOAc through the initial formation of neutral [(L-TMS)Au(OAc)]. The addition of excess $AgSbF_6$ to a solution of **8** in CH_2Cl_2 led quantitively to the formation of cluster **4c**.

We confirmed that the reaction of [Ph_3PAuCl] with Ag_2O and $AgSbF_6$ gives oxonium gold cluster [$O(AuPPh_3)_3$](SbF_6),[21] which suggests that similar oxonium gold complexes might be involved as intermediates in the formation of the gold–silver clusters. Indeed, upon addition of $AgSbF_6$ to a mixture of **1a** and Ag_2O in CD_2Cl_2, a new species corresponding to **9a** was formed, which reacted further to finally form **4a** (Scheme 5). Oxonium gold cluster **9a** was isolated as a white solid and its structure was confirmed by mass spectrometry (*m/z* 1609.2049). Starting from **1d**, a similar oxonium trigold(I) complex **9d** was obtained, whose structure was determined by X-ray diffraction.[15,22]

Presumably, reaction of **1a–d** complexes with AgX salts leads to complexes [(L-TMS)Au(S)]$^+X^-$, which immediately evolve to form hexanuclear gold(I) clusters **2a–d**. On the other hand, when the reactions are performed in the presence of Ag_2O, oxonium trigold complexes **9** are formed as intermedi-

ates, which are less reactive in the C–Si auration and, as a result, can incorporate silver(I) leading to the formation of gold(I)–silver(I) clusters.

Hexagold clusters **2a–d** are stable in solution. Thus, cluster **2a** was recovered unchanged upon recrystallization in acetonitrile as well as after being heated at 80 °C in 1,2-dichloroethane for 24 h. Thermogravimetric analysis shows that clusters **2a**, **2e**, **3a**, and **4a** only undergo decomposition in the solid state at high temperatures (230–270 °C).[23] However, treatment of **2a** with PPh_3 in CH_2Cl_2 led to the formation of a known digold complex similar to **8**.[19] In the case of pentagold cluster **6**, the ^{31}P NMR signals became broad in acetonitrile solution, although **6** was recovered unchanged after crystallization in this solvent.

The catalytic activity of the new clusters was studied in the addition of 1,3,5-trimethoxybenzene, indole, and *N*-methylindole to 1,6-enyne **10** to give cycloadducts **11a–b** regio- and stereoselectively (Table 1).[24] Clusters **2a–e** showed activities in the order **2e** > **2c** > **2a** ≈ **2b** > **2d** (Table 1, entries 1–9). These results correlate with the electronic and steric properties of the ligands, since 2-furyl group in **1e** is the most electron-withdrawing and less bulky phosphine substituent. Remarkably, 1 mol% of cluster **2e** led to **11a** in 95% yield in about 3 h (entry 7), showing a catalytic activity comparable to that displayed by a bulky phosphite gold(I) complex (5 mol%, 2 h, 66% yield),[24] which is one of the most reactive gold(I) complexes used routinely in the activation of alkynes. The catalyst loading with **2a** and **2d** could be decreased to 0.05 mol%

Table 1. Addition of aromatic and heteroaromatic nucleophiles to 1,6-enyne **10** to form **11a–c** catalyzed by gold or gold–silver clusters.

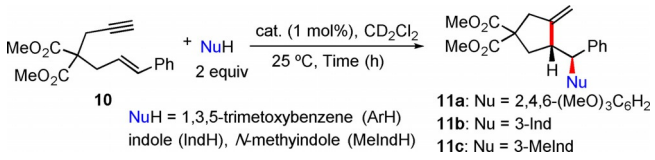

10

NuH = 1,3,5-trimetoxybenzene (ArH)
indole (IndH), *N*-methyindole (MeIndH)

11a: Nu = 2,4,6-$(MeO)_3C_6H_2$
11b: Nu = 3-Ind
11c: Nu = 3-MeInd

Entry	NuH	Catalyst	Time [h]	**11a–c** (yield, %)[a]
1	ArH	**2a**	20	**11a** (76)
2	IndH	**2a**	20	**11b** (40)
3	MeIndH	**2a**	16	**11c** (76)
4	ArH	**2b**	12	**11a** (71)
5	ArH	**2c**	12	**11a** (87)
6	ArH	**2d**	12	**11a** (3)
7	ArH	**2e**	3.3	**11a** (98, 95[b])
8	IndH	**2e**	8	**11b** (79)
9	MeIndH	**2e**	8	**11c** (67)
10	ArH	**4a**	4	**11a** (98)
11	ArH	**3a**	4.5	**11a** (97)
12	ArH	**3b**	9	**11a** (99)
13	ArH	**4c**	6.5	**11a** (96)
14	ArH	**6**	12	**11a** (< 1)
15[c]	ArH	**6** + $NaBAr^F_4$	12	**11a** (99)
16	ArH	**7**	12	–[d]
17[c]	ArH	**7** + $NaBAr^F_4$	12	–[d]
18	ArH	**8**	24	–[d]
19	ArH	**5a**[e]	3.5	**11a** (93)

[a] Yields determined by ^1H NMR using 1,3,5-tris(trifluoromethyl)benzene as internal standard. [b] Isolated yield. [c] Reaction in the presence of $NaBAr^F_4$ (10 mol%). [d] < 1% yield. [e] Catalyst loading 0.05%.

maintaining good conversions.[23] Cluster **2e** was also found to be the most reactive[23] for the formation of indenes from 7-phenylethynyl cycloheptatriene,[25] and for the formal [4+2] intramolecular cycloaddition of arylalkynes with alkenes.[26]

Clusters **3a,b** and **4a,c** display higher catalytic activity than the corresponding hexagold congeners probably due to the structure effect by silver doping[27] (Table 1, entries 10–11). In contrast, the reaction with cluster **6** led only to traces of **11a** (entry 14), although the reactivity could be restored in the presence of $NaBAr^F_4$ (entry 15), whereas $NaBAr^F_4$ by itself does not promote this transformation. However, cluster **7** was unreactive even in the presence of $NaBAr^F_4$ (entries 16 and 17). Digold complex **8** showed no reactivity (entry 18). Hexadecanuclear cluster **5a** $[Au_{12}Ag_4]$ also displays good activity (0.05 mol%, 3.5 h, 93% yield of **20a**) (entry 19). Similar catalytic activity was found with enynes bearing internal alkynes.[23]

Homometallic gold clusters **2a–c**, **2d,** and **6** did not undergo decomposition when the corresponding reactions in Table 1 were monitored by ^{31}P NMR spectroscopy.[23] On the other hand, the gold(I)–silver(I) clusters underwent slow decomposition, which might explain why heteronuclear clusters **4a** and **4c**, which present only PAu–Ag–AuP motifs, are also catalytically active (entries 10 and 13). In these cases, as suggested by ^{31}P NMR, decomposition or structural rearrangement of **4a** and **4c** to generate an active gold(I) species probably takes place in solution.

To probe our hypothesis that the catalytically active site is the central gold atom in the PAu–Au–AuP structural motifs, we also examined the reactivity of known full-phosphine-protected gold and gold–silver clusters $[Au_6C]$,[16a] $[Au_6Ag_4C]$,[16b] nanogold clusters nano-$[Au_6]$[19] and $[Au_{13}]$.[28] However, none of these species displayed catalytic activity in the addition of 1,3,5-trimethoxybenzene to 1,6-enyne **10** at 25 °C.[23]

Conclusions

We have found that the auration of trimethylsilyl phosphines leads to the formation of well-defined small gold and gold–silver clusters containing 3c–2e Au–C–M (M = Au/Ag) bonds. On the other hand, when the chloride abstraction of complexes [(L–TMS)AuCl] was performed with $AgSbF_6$ in the presence of Ag_2O, hexanuclear gold–silver clusters $[Au_4Ag_2]^{2+}$ were obtained. Trinuclear oxonium gold species $[Au_3O]^+$ acts as the intermediate in this silver-doping process, which takes place due to a slower C–Si auration process. Other clusters $[Au_5]$, $[Au_4Ag]$, $[Au_2]$ and $[Au_{12}Ag_4]$ have also been obtained. The activity of these small gold clusters has been studied in typical Au^I-catalyzed reactions of enynes. Remarkably, hexanuclear gold cluster **2e** with difurylphosphine ligand displays a reactivity similar or even higher than other commonly used mononuclear gold catalysts.

Acknowledgements

We thank MINECO/FEDER, UE (CTQ2016-75960-P), the European Research Council (Advanced Grant No. 835080), H2020-

Marie Sklodowska-Curie contract to X.-L. Pei (Grant Agreement: 747170), the AGAUR (2017 SGR 1257), and CERCA Program/ Generalitat de Catalunya for financial support. We thank Shaofei Ni for the optimization of the structure of **9a** by DFT calculations and Mauro Mato for helpful discussions. We also thank the ICIQ X-ray diffraction unit for the crystallographic analysis.

Conflict of interest

The authors declare no conflict of interest.

Keywords: C(sp^2)–Si auration · gold catalysis · gold clusters · metalophilic interactions · silver–gold clusters

[1] M. C. Gimeno, *Modern Supramolecular Gold Chemistry: Gold–Metal Interactions and Applications* (Ed.: A. Laguna), Wiley-VCH, Weinheim, **2008**, pp. 1–63.
[2] a) C.-M. Che, S.-W. Lai, *Coord. Chem. Rev.* **2005**, *249*, 1296–1309; b) M. C. Gimeno, A. Laguna, *Chem. Soc. Rev.* **2008**, *37*, 1952–1966; c) V. W.-W. Yam, V. K.-M. Au, S. Y.-L. Leung, *Chem. Rev.* **2015**, *115*, 7589–7728.
[3] a) G. Li, R. Jin, *Acc. Chem. Res.* **2013**, *46*, 1749–1758; b) L. Liu, A. Corma, *Chem. Rev.* **2018**, *118*, 4981–5079.
[4] a) J. Oliver-Meseguer, J. R. Cabrero-Antonino, I. Dominguez, A. Leyva-Pérez, A. Corma, *Science* **2012**, *338*, 1452–1455; b) J. Oliver-Meseguer, A. Leyva-Pérez, A. Corma, *ChemCatChem* **2013**, *5*, 3509–3515; c) L. Jin, D. S. Weinberger, M. Melaimi, C. E. Moore, A. L. Rheingold, G. Bertrand, *Angew. Chem. Int. Ed.* **2014**, *53*, 9059–9063; *Angew. Chem.* **2014**, *126*, 9205–9209; d) J. Cordón, G. Jiménez-Osés, J. M. López de Luzuriaga, M. Monge, *Nat. Commun.* **2017**, *8*, 1657–1664.
[5] S. M. Lang, T. M. Bernhardt, V. Chernyy, J. M. Bakker, R. N. Barnett, U. Landman, *Angew. Chem. Int. Ed.* **2017**, *56*, 13406–13410; *Angew. Chem.* **2017**, *129*, 13591–13595.
[6] P. H. Y. Cheong, P. Morganelli, M. R. Luzung, K. N. Houk, F. D. Toste, *J. Am. Chem. Soc.* **2008**, *130*, 4517–4526.
[7] E. S. Smirnova, J. M. Muñoz Molina, A. Johnson, N. A. Bandeira, C. Bo, A. M. Echavarren, *Angew. Chem. Int. Ed.* **2016**, *55*, 7487–7491; *Angew. Chem.* **2016**, *128*, 7613–7617.
[8] a) H. Yu, B. Rao, W. Jiang, S. Yang, M. Zhu, *Coord. Chem. Rev.* **2019**, *378*, 595–617; b) Z. Lei, Q.-M. Wang, *Coord. Chem. Rev.* **2019**, *378*, 382–394.
[9] Au^I clusters: a) Z. N. Chen, N. Zhao, Y. Fan, J. Ni, *Coord. Chem. Rev.* **2009**, *253*, 1–20; b) M. C. Blanco, J. Cámara, M. C. Gimeno, A. Laguna, S. L. James, M. C. Lagunas, M. D. Villacampa, *Angew. Chem. Int. Ed.* **2012**, *51*, 9777–9779; *Angew. Chem.* **2012**, *124*, 9915–9917; c) Au^I–Au^0 nanoclusters: G. Soldan, M. A. Aljuhani, M. S. Bootharaju, L. G. AbdulHalim, M. R. Parida, A. Emwas, O. F. Mohammed, O. M. Bakr, *Angew. Chem. Int. Ed.* **2016**, *55*, 5749–5753; *Angew. Chem.* **2016**, *128*, 5843–5847; d) T. Chen, S. Yang, J. Chai, Y. Song, J. Fan, B. Rao, H. Sheng, H. Yu, M. Zhu, *Sci. Adv.* **2017**, 1700956; e) Z. Lei, X.-K. Wan, S.-F. Yuan, Z.-J. Guan, Q.-M. Wang, *Acc. Chem. Res.* **2018**, *51*, 2465–2474; f) M. Iwasaki, Y. Shichibu, K. Konishi, *Angew. Chem. Int. Ed.* **2019**, *58*, 2443–2447; *Angew. Chem.* **2019**, *131*, 2465–2469.
[10] a) X.-L. Pei, Y. Yang, Z. Lei, Q.-M. Wang, *J. Am. Chem. Soc.* **2013**, *135*, 6435–6437; b) J. R. Shakirova, E. V. Grachova, A. J. Karttunen, V. V. Gurzhiy, S. P. Tunik, I. O. Koshevoy, *Dalton Trans.* **2014**, *43*, 6236–6243; c) X.-L. Pei, Y. Yang, Z. Lei, S.-S. Chang, Z.-J. Guan, X.-K. Wan, T.-B. Wen, Q.-M. Wang, *J. Am. Chem. Soc.* **2015**, *137*, 5520–5525; d) X. He, Y. Wang, H. Jiang, L. Zhao, *J. Am. Chem. Soc.* **2016**, *138*, 5634–5643.
[11] E. S. Smirnova, A. M. Echavarren, *Angew. Chem. Int. Ed.* **2013**, *52*, 9023–9026; *Angew. Chem.* **2013**, *125*, 9193–9196.
[12] a) M. P. Robinson, G. C. Lloyd-Jones, *ACS Catal.* **2018**, *8*, 7484–7488; b) M. Olaru, E. Rychagova, S. Ketkov, Y. Shynkarenko, S. Yakunin, M. V. Kovalenko, A. Yablonskiy, B. Andreev, F. Kleemiss, J. Beckmann, M. Vogt, *J. Am. Chem. Soc.* **2020**, *142*, 373–381; c) M. Olaru, J. F. Kögel, R. Aoki, R. Sakamoto, H. Nishihara, E. Lork, S. Mebs, M. Vogt, J. Beckmann, *Chem. Eur. J.* **2020**, *26*, 275–284.
[13] a) E. J. Fernández, A. Laguna, J. M. López de Luzuriaga, M. Montiel, M. E. Olmos, J. Pérez, R. C. Puelles, *Organometallics* **2006**, *25*, 4307–4315; b) T. Lasanta, M. E. Olmos, A. Laguna, J. M. López de Luzuriaga, P. Naumov, *J. Am. Chem. Soc.* **2011**, *133*, 16358–16361.
[14] Recent papers on Au_{25}: a) P. N. Gunawardene, J. F. Corrigan, M. S. Workentin, *J. Am. Chem. Soc.* **2019**, *141*, 11781–11785; b) X. Cai, G. Saranya, K. Shen, M. Chen, R. Si, W. Ding, Y. Zhu, *Angew. Chem. Int. Ed.* **2019**, *58*, 9964–9968; *Angew. Chem.* **2019**, *131*, 10069–10073; c) Z. Huang, Y. Ishida, T. Yonezawa, *Angew. Chem. Int. Ed.* **2019**, *58*, 13411–13415; *Angew. Chem.* **2019**, *131*, 13545–13549; d) H. Shen, G. Deng, S. Kaappa, T. Tan, Y.-Z. Han, S. Malola, S.-C. Lin, B. K. Teo, H. Häkkinen, N. Zheng, *Angew. Chem. Int. Ed.* **2019**, *58*, 17731–17735; *Angew. Chem.* **2019**, *131*, 17895–17899.
[15] CCDC 1940384 (**1a**), 1940380 (**1b**), 1940383 (**1c**), 1940377 (**1d**), 1940378 (**1e**), 1940374 (**2b**), 1940376 (**2c**), 1940382 (**2d**), 1940372 (**2e**), 1940385 (**3a**·acetone), 1940373 (**3a**·MeOH), 1936590 (**3b**), 1940379 (**4a**), 1940367 (**4c**), 1940375 (**5a′**), 1940371 (**6**), 1940370 (**7**), 1940367 (**8**), and 1940368 (**9d**) contain the supplementary crystallographic data for this paper. These data are provided free of charge by The Cambridge Crystallographic Data Centre.
[16] a) F. Scherbaum, A. Grohmann, B. Huber, C. Krüger, H. Schmidbaur, *Angew. Chem. Int. Ed. Engl.* **1988**, *27*, 1544–1546; *Angew. Chem.* **1988**, *100*, 1602–1604; b) J.-H. Jia, Q.-M. Wang, *J. Am. Chem. Soc.* **2009**, *131*, 16634–16635; c) Y. Yang, X.-L. Pei, Q.-M. Wang, *J. Am. Chem. Soc.* **2013**, *135*, 16184–16191; d) X.-Y. Liu, Y. Yang, Z. Lei, Z.-J. Guan, Q.-M. Wang, *Chem. Commun.* **2016**, *52*, 8022–8025; e) H. Ube, Q. Zhang, M. Shionoya, *Organometallics* **2018**, *37*, 2007–2009.
[17] C. E. Briant, K. P. Hall, D. M. P. Mingos, A. C. Wheeler, *J. Chem. Soc. Dalton Trans.* **1986**, 687–692.
[18] a) H. Schmidbaur, S. Hofreiter, M. Paul, *Nature* **1995**, *377*, 503–504; b) N. Kenji, Y. Takuya, S. Yoshitaka, N. Arisa, T. Shinichiro, *Inorg. Chem.* **2010**, *49*, 8247–8254.
[19] M. A. Bennett, L. L. Welling, A. C. Willis, *Inorg. Chem.* **1997**, *36*, 5670–5672.
[20] M. A. Bennett, S. K. Bhargava, K. D. Griffiths, G. B. Robertson, W. A. Wickramasinghe, A. C. Willis, *Angew. Chem. Int. Ed. Engl.* **1987**, *26*, 258–260; *Angew. Chem.* **1987**, *99*, 261–262.
[21] A. N. Nesmeyanov, E. G. Perevalova, Y. T. Struchkov, M. Y. Antipin, K. I. Grandberg, V. P. Dyadhenko, *J. Organomet. Chem.* **1980**, *201*, 343–349.
[22] a) Due to the high symmetry of space group, the anion cannot be confirmed clearly by X-ray analysis. Other related complexes $[OAu_3(L)_3](X)$ have been also characterized by HRMS; b) The calculated structure of **9a** was optimized using the B3LYP density functional with the Gaussian 09 program. The basis set 6-31G* was used for the C, H, O, P, Si, and the LANl2DZ was used for Au. See the Supporting Information for additional details.
[23] See details in the Supporting Information.
[24] a) P. Y. Toullec, E. Genin, L. Leseurre, J. P. Genêt, V. Michelet, *Angew. Chem. Int. Ed.* **2006**, *45*, 7427–7430; *Angew. Chem.* **2006**, *118*, 7587–7590; b) C. H. M. Amijs, C. Ferrer, A. M. Echavarren, *Chem. Commun.* **2007**, 698–700; c) P. Y. Toullec, C. M. Chao, Q. Chen, S. Gladiali, J. P. Genet, V. Michelet, *Adv. Synth. Catal.* **2008**, *350*, 2401–2408; d) C. H. Amijs, V. López-Carrillo, M. Raducan, P. Pérez-Galán, C. Ferrer, A. M. Echavarren, *J. Org. Chem.* **2008**, *73*, 7721–7730; e) A. Pradal, C. M. Chao, M. R. Vitale, P. Y. Toullec, V. Michelet, *Tetrahedron* **2011**, *67*, 4371–4377.
[25] P. R. McGonigal, C. de León, Y. Wang, A. Homs, C. R. Solorio-Alvarado, A. M. Echavarren, *Angew. Chem. Int. Ed.* **2012**, *51*, 13093–13096; *Angew. Chem.* **2012**, *124*, 13270–13273.
[26] a) C. Nieto-Oberhuber, S. López, A. M. Echavarren, *J. Am. Chem. Soc.* **2005**, *127*, 6178–6179; b) C. Nieto-Oberhuber, P. Pérez-Galán, E. Herrero-Gómez, T. Lauterbach, C. Rodríguez, S. López, C. Bour, A. Rosellón, D. J. Cárdenas, A. M. Echavarren, *J. Am. Chem. Soc.* **2008**, *130*, 269–279.
[27] S. Wang, S. Jin, S. Yang, S. Chen, Y. Song, J. Zhang, M. Zhu, *Science Adv.* **2015**, 1500441.
[28] Y.-Z. Li, W. K. Leong, *RSC Adv.* **2019**, *9*, 5475–5479.

Manuscript received: March 29, 2020
Accepted manuscript online: March 31, 2020
Version of record online: May 11, 2020

